AIMS Mathematics

http://www.aimspress.com/journal/Math

AIMS Mathematics, 9(2): 4684–4706.
DOI:10.3934/math.2024226
Received: 28 November 2023
Revised: 07 January 2024
Accepted: 15 January 2024
Published: 19 January 2024

Research article

Stability and bifurcation analysis of a discrete Leslie predator-prey system via piecewise constant argument method

Saud Fahad Aldosary[1] **and Rizwan Ahmed**[2,*]

[1] Department of Mathematics, College of Science and Humanities in Alkharj, Prince Sattam bin Abdulaziz University, Alkharj 11942, Saudi Arabia

[2] Department of Mathematics, Air University Multan Campus, Multan, Pakistan

* **Correspondence:** Email: rizwanahmed488@gmail.com.

Abstract: The objective of this study was to analyze the complex dynamics of a discrete-time predator-prey system by using the piecewise constant argument technique. The existence and stability of fixed points were examined. It was shown that the system experienced period-doubling (PD) and Neimark-Sacker (NS) bifurcations at the positive fixed point by using the center manifold and bifurcation theory. The management of the system's bifurcating and fluctuating behavior may be controlled via the use of feedback and hybrid control approaches. Both methods were effective in controlling bifurcation and chaos. Furthermore, we used numerical simulations to empirically validate our theoretical findings. The chaotic behaviors of the system were recognized through bifurcation diagrams and maximum Lyapunov exponent graphs. The stability of the positive fixed point within the optimal prey growth rate range $A_1 < a < A_2$ was highlighted by our observations. When the value of a falls below a certain threshold A_1, it becomes challenging to effectively sustain prey populations in the face of predation, thereby affecting the survival of predators. When the growth rate surpasses a specific threshold denoted as A_2, it initiates a phase of rapid expansion. Predators initially benefit from this phase because it supplies them with sufficient food. Subsequently, resource depletion could occur, potentially resulting in long-term consequences for populations of both the predator and prey. Therefore, a moderate amount of prey's growth rate was beneficial for both predator and prey populations.

Keywords: predator-prey; Leslie-Gower; piecewise-constant argument method; stability; bifurcation; chaos control
Mathematics Subject Classification: 39A28, 39A30

1. Introduction

As a fundamental component of ecological investigation, the interaction between predator and prey populations in biological ecosystems has long been a subject of interest and analysis among biologists and mathematicians. Predator-prey systems involve the dynamic interaction of two populations, in which the survival of one species (the predators) is dependent on the consumption of another species (the prey). A number of researchers have conducted thorough investigations and analyses of diverse mathematical frameworks that explicate the interrelationships between species. The fundamental objective of these inquiries has been to examine the complex and varied dynamics that are intrinsic to these systems. The primary areas of concern include stability analysis, limit cycles, bifurcations, chaotic phenomena, and associated phenomena [1–8].

The Lotka-Volterra system, which is the classic predator-prey framework, was initially proposed and established by Volterra and Lotka [9, 10]. Within the conceptual framework of this system, it is postulated that all components adhere to linear functions, including the growth rate, predator mortality rate, and the transformation of prey biomass into predator reproduction. However, it is crucial to acknowledge that nonlinear components exert a substantial influence on predator-prey dynamics that occur in nature. Scholars have suggested numerous improvements to address the system's inability to incorporate specific real-world events. Leslie and Gower [11, 12] introduced the classical Leslie-Gower predator-prey system to provide a comprehensive representation of the real-world scenario. This system incorporates the notion that the predator's environmental carrying capacity is directly proportional to the population density of the prey. Britton [13] suggested the following Leslie's system:

$$\begin{cases} \frac{dx}{dt} = ax - bx^2 - cxy, \\ \frac{dy}{dt} = dy - \frac{\alpha y^2}{x}, \end{cases} \tag{1.1}$$

where x and y represent the population densities of prey and predator, respectively. The parameter a denotes the intrinsic growth rate of prey, while b quantifies the strength of competition among individuals of prey. The rate of change due to interaction is represented by the parameter c. Additionally, the intrinsic growth rate of the predator is denoted by d and α signifies the density of prey required to sustain a single predator. All parameters a, b, c, d and α are positive constants.

There are two distinct categories of modeling methodologies, namely, discrete-time systems and continuous-time systems. Much research has been dedicated to examining the nonlinear dynamical characteristics of continuous systems. In contrast, the investigation of discrete systems has been relatively limited. Nevertheless, over time scholars have come to recognize that discrete systems possess distinct dynamical qualities when compared to their continuous counterparts. The discrete-time systems provide the most accurate description of the dynamics exhibited by animals that engage in seasonal reproduction and have nonoverlapping generations. Furthermore, as compared to continuous-time systems, these discrete systems demonstrate much more complicated dynamical patterns [14–21]. Hence, discrete systems possess more attraction in comparison to continuous systems. It is crucial to use suitable numerical techniques for discretizing the continuous systems. The forward Euler strategy [22–26] has been widely used due to its simplicity. However, there needs to be more dynamic consistency when comparing the discrete version to its continuous equivalents. The discrete system produced by the use of the Euler approach lacks realism. Certain parameters and initial values may attribute the presence of negative values for the prey and predator population sizes. Nevertheless, using the piecewise constant argument approach [27–30] eliminates negative values. Khan et al. [31] investigated the discrete form of the system (1.1) as follows:

$$\begin{cases} x_{n+1} = (1+ah)x_n - bhx_n^2 - chx_ny_n, \\ y_{n+1} = \frac{(1+dh)x_ny_n - \alpha hy_n^2}{x_n}. \end{cases} \tag{1.2}$$

They obtained the discretization using the forward Euler technique. They investigated stability analysis and demonstrated the occurrence of the Neimark-Sacker (NS) bifurcation in the system. The authors used the hybrid control methodology to regulate the chaotic behavior in the system. In this study, we use the piecewise constant argument as an alternative method for discretizing the continuous-time system (1.1). By utilizing piecewise constant arguments to solve nonlinear differential equations and considering the regular time interval for the average growth rate in both populations, we can rewrite system (1.1) as follows:

$$\begin{cases} \frac{1}{x(t)}\frac{dx}{dt} = a - bx[t] - cy[t], \\ \frac{1}{y(t)}\frac{dy}{dt} = d - \frac{\alpha y[t]}{x[t]}, \end{cases} \tag{1.3}$$

where $[t]$ represents the integer part of t and $0 < t < \infty$. Furthermore, integrating system (1.3) on an interval $[n, n+1)$ with $n = 0, 1, 2, \cdots$ yields the following system:

$$\begin{cases} x(t) = x_n e^{\left(a - bx_n - cy_n\right)(t-n)}, \\ y(t) = y_n e^{\left(d - \frac{\alpha y_n}{x_n}\right)(t-n)}. \end{cases} \tag{1.4}$$

Taking $t \to n+1$, we obtain the following discrete-time system:

$$\begin{cases} x_{n+1} = x_n e^{a - bx_n - cy_n}, \\ y_{n+1} = y_n e^{d - \frac{\alpha y_n}{x_n}}. \end{cases} \tag{1.5}$$

The subsequent sections of the paper are structured in the following manner: The objective of Section 2 is to investigate the presence and topological classification of fixed points. Section 3 provides a comprehensive examination of the bifurcation analysis pertaining to the period-doubling (PD) and NS bifurcations occurring at the positive fixed point. Section 4 employs two control methodologies in order to effectively regulate bifurcations and chaos. In order to validate and explicate the theoretical findings, numerical examples are presented in Section 5. The analysis performed in this research is ultimately summarized in Section 6.

2. Topolgical classification of fixed points

The understanding of fixed point stability holds significant importance within the context of a predator-prey system. The fixed points represent equilibrium states wherein the populations of predators and prey have achieved a condition of balance. By conducting an analysis of their stability, we are able to make predictions about the long-term patterns exhibited by these ecological systems, gaining a deeper understanding of the various factors that contribute to the overall dynamics of the ecosystem.

2.1. Existence of fixed points

The fixed points for system (1.5) can be obtained by solving

$$\begin{cases} x = xe^{a-bx-cy}, \\ y = ye^{d-\frac{\alpha y}{x}}, \end{cases} \tag{2.1}$$

for x and y. It is obtained that system (1.5) has two fixed points $E_1 = (\frac{a}{b}, 0), E_2 = (\frac{a\alpha}{cd+b\alpha}, \frac{ad}{cd+b\alpha})$.

2.2. Stability of fixed points

To classify the fixed points, we employ the following results.

Lemma 2.1. *[32] Let $\Lambda(\xi) = \xi^2 + K_1\xi + K_0$ be the characteristic polynomial of Jacobian matrix computed at fixed point (x, y) and ξ_1, ξ_2 satisfy $\Lambda(\xi) = 0$, then (x, y) is a*
(1) sink (locally asymptotically stable (LAS)) when $|\xi_1| < 1$ along with $|\xi_2| < 1$,
(2) source when $|\xi_1| > 1$ along with $|\xi_2| > 1$,
(3) saddle point (SP) when $|\xi_1| < 1$ and $|\xi_2| > 1$ (or $|\xi_1| > 1$ and $|\xi_2| < 1$),
(4) non-hyperbolic point (NHP) when the modulus of either of ξ_1 and ξ_2 is one.

Lemma 2.2. *[32] Consider the quadratic function $\Lambda(\xi) = \xi^2 + K_1\xi + K_0$. Suppose that $\Lambda(1) > 0$. If ξ_1 and ξ_2 both satisfy the equation $\Lambda(\xi) = 0$, then*
(1) $|\xi_1| < 1$ along with $|\xi_2| < 1$ if $\Lambda(-1) > 0$ and $K_0 < 1$,
(2) $|\xi_1| < 1$ and $|\xi_2| > 1$ (or $|\xi_1| > 1$ and $|\xi_2| < 1$) if $\Lambda(-1) < 0$,
(3) $|\xi_{1,2}| > 1$ if $\Lambda(-1) > 0$ and $K_0 > 1$,
(4) $|\xi_2| \neq 1$ and $\xi_1 = -1$ if $\Lambda(-1) = 0$ and $K_1 \neq 0, 2$,
(5) $\xi_1, \xi_2 \in \mathbb{C}$ along with $|\xi_{1,2}| = 1$ if $K_1^2 - 4K_0 < 0$ and $K_0 = 1$.

Through simple computations, one can obtain the Jacobian matrix at an arbitrary fixed point (x, y) as follows:

$$J(x, y) = \begin{bmatrix} e^{a-bx-cy}(1 - bx) & -ce^{a-bx-cy}x \\ \frac{e^{d-\frac{y\alpha}{x}} y^2\alpha}{x^2} & \frac{e^{d-\frac{y\alpha}{x}} (x-y\alpha)}{x} \end{bmatrix}.$$

The Jacobian matrix of system (1.5) computed at E_1 is shown as follows:

$$J(E_1) = \begin{bmatrix} 1 - a & -\frac{ac}{b} \\ 0 & e^d \end{bmatrix}.$$

Also, the Jacobian matrix at E_2 is given by

$$J(E_2) = \begin{bmatrix} 1 - \frac{ab\alpha}{cd+b\alpha} & -\frac{ac\alpha}{cd+b\alpha} \\ \frac{d^2}{\alpha} & 1 - d \end{bmatrix}. \tag{2.2}$$

Proposition 2.1. *The boundary fixed point E_1 is*
(1) never LAS,
(2) a source if $a > 2$,
(3) SP if $0 < a < 2$,
(4) NHP if $a = 2$.

Next, we classify the positive fixed point E_2 of system (1.5) according to the above Jacobian matrix and Lemma 2.2. We obtain

$$J(E_2)=\begin{bmatrix}1-\frac{ab\alpha}{cd+b\alpha} & -\frac{ac\alpha}{cd+b\alpha}\\ \frac{d^2}{\alpha} & 1-d\end{bmatrix}. \tag{2.3}$$

The characteristic polynomial of $J(E_2)$ is

$$\Lambda(\xi)=\xi^2+\Big(-2+d+\frac{ab\alpha}{cd+b\alpha}\Big)\xi+(-1+a)(-1+d)+\frac{acd}{cd+b\alpha}.$$

It can be obtained through calculations that

$$\Lambda(0)=(-1+a)(-1+d)+\frac{acd}{cd+b\alpha},\ \Lambda(-1)=(-2+a)(-2+d)+\frac{2acd}{cd+b\alpha},\ \Lambda(1)=ad.$$

Theorem 2.1. *The following holds for the interior fixed point E_2 of the system* (1.5)*:*

(1) E_2 is a sink if one of the following conditions holds:

(a) $d<2$ and if one of the following conditions holds:

(i) $b+\frac{c(-4+d)d^2}{(-2+d)^2\alpha}\le 0$ and $a<\frac{d(cd+b\alpha)}{cd^2+b(-1+d)\alpha}$,

(ii) $b+\frac{c(-4+d)d^2}{(-2+d)^2\alpha}>0$ and $a<\frac{2(-2+d)(cd+b\alpha)}{cd^2+(-2+d)\alpha}$,

(b) $d=2$ and $a<\frac{4c+2b\alpha}{4c+b\alpha}$,

(c) $2<d<4, b+\frac{c(-4+d)d^2}{(-2+d)^2\alpha}<0$, and

$$\frac{2(-2+d)(cd+b\alpha)}{cd^2+(-2+d)\alpha}<a<\frac{d(cd+b\alpha)}{cd^2+b(-1+d)\alpha},$$

(2) E_2 is a saddle point if one of the following conditions holds:

(a) $0<d<2, b>\frac{cd^2}{(2-d)\alpha}$, and $a>\frac{2(-2+d)(cd+b\alpha)}{cd^2+b(-2+d)\alpha}$,

(b) $d>2$ and $0<a<\frac{2(-2+d)(cd+b\alpha)}{cd^2+b(-2+d)\alpha}$,

(3) E_2 is a source if one of the following conditions holds:

(a) $d=2$ and $a>\frac{4c+2b\alpha}{4c+b\alpha}$,

(b) $d>4$ and $a>\frac{2(-2+d)(cd+b\alpha)}{cd^2+b(-2+d)\alpha}$,

(c) $a>\frac{d(cd+b\alpha)}{cd^2+b(-1+d)\alpha}$ and if one of the following conditions holds:

(i) $0<d<2$ and $b\ge\frac{cd^2}{(2-d)\alpha}$,

(ii) $2<d\le 4$ and $b+\frac{c(-4+d)d^2}{(-2+d)^2\alpha}\le 0$,

(d) $d<2, \frac{cd^2}{(2-d)\alpha}<b<-\frac{c(-4+d)d^2}{(-2+d)^2\alpha}$ and

$$\frac{d(cd+b\alpha)}{cd^2+b(-1+d)\alpha}<a<\frac{2(-2+d)(cd+b\alpha)}{cd^2+b(-2+d)\alpha},$$

(e) $2<d\le 4, b+\frac{c(-4+d)d^2}{(-2+d)^2\alpha}>0$, and $a>\frac{2(-2+d)(cd+b\alpha)}{cd^2+b(-2+d)\alpha}$,

(4) E_2 is non-hyperbolic point and experiences PD bifurcation if $a=A_1=\frac{2(-2+d)(cd+b\alpha)}{cd^2+b(-2+d)\alpha}$ and if one of the requirements listed below is satisfied:

(a) $b+\frac{c(-4+d)d^2}{(-2+d)^2\alpha}<0$ and if one of the following conditions holds:

(i) $2<d\le 4$,

(ii) $d < 2$ *and* $b > \frac{cd^2}{(2-d)\alpha}$,

(b) $d \in (0, 2) \cup (2, 4]$ *and* $b + \frac{c(-4+d)d^2}{(-2+d)^2\alpha} > 0$,

(c) $d > 4$,

(5) E_2 *is non-hyperbolic point and experiences NS bifurcation if* $a = A_2 = \frac{d(cd+b\alpha)}{cd^2+b(-1+d)\alpha}$ *and if one of the requirements listed below is satisfied:*

(a) $d = 2$,

(b) $d \in (0, 2) \cup (2, 4)$ *and* $b + \frac{c(-4+d)d^2}{(-2+d)^2\alpha} < 0$.

3. Bifurcation analysis

This section is focused on conducting a comprehensive investigation of the bifurcation phenomenon involving PD and NS bifurcation in the system (1.5) at the positive fixed point E_2. In order to obtain a thorough treatment of bifurcation analysis, we recommend that readers refer to [33, 34]. The bifurcation holds significant implications for the dynamics of the system, shedding light on scenarios where even slight modifications to parameters yield substantial alterations in the dynamics of predator-prey relationships. In addition, gaining knowledge about PD and NS bifurcations contributes to a deeper comprehension of ecosystem dynamics. This understanding, in turn, facilitates the formulation of effective conservation and management strategies aimed at sustaining the enduring coexistence of predator and prey populations. This study initiates by investigating the PD bifurcation at E_2 based on condition (4-c) as presented in Theorem 2.1. By applying a small perturbation δ ($|\delta| \lll 1$) to the bifurcation parameter around the critical value A_1, the system (1.5) is changed to

$$\begin{cases} x_{n+1} = x_n e^{(A_1+\delta)-bx_n-cy_n}, \\ y_{n+1} = y_n e^{d-\frac{\alpha y_n}{x_n}}. \end{cases} \tag{3.1}$$

We transform the fixed point E_2 to the origin by considering the change of variables $u_n = x_n - \frac{(a+\delta)\alpha}{cd+b\alpha}$, $v_n = y_n - \frac{(a+\delta)d}{cd+b\alpha}$. As a result, the system (3.1) is transformed into the following form:

$$\begin{bmatrix} u_{n+1} \\ v_{n+1} \end{bmatrix} = \begin{bmatrix} \frac{cd^2-b(-2+d)\alpha}{cd^2+b(-2+d)\alpha} & -\frac{2c(-2+d)\alpha}{cd^2+b(-2+d)\alpha} \\ \frac{d^2}{\alpha} & 1-d \end{bmatrix} \begin{bmatrix} u_n \\ v_n \end{bmatrix} + \begin{bmatrix} F(u_n, v_n, \delta) \\ G(u_n, v_n, \delta) \end{bmatrix}, \tag{3.2}$$

where

$$\begin{aligned} F(u_n, v_n, \delta) &= a_1u_n^2 + a_2u_n^2v_n + a_3v_n^2 + a_4v_n^3 + a_5u_nv_n^2 + a_6u_nv_n + a_7u_n^3 + a_8u_n\delta + a_9v_n\delta \\ &\quad + a_{10}u_nv_n\delta + a_{11}u_n^2\delta + a_{12}v_n^2\delta + O((|u_n| + |v_n| + |\delta|)^4), \\ G(u_n, v_n, \delta) &= b_1v_n^2 + b_2u_nv_n + b_3v_n^3 + b_4u_n^2v_n + b_5u_nv_n^2 + b_6u_n^3 + b_7u_n^2 + b_8v_n^2\delta + b_9u_nv_n\delta \\ &\quad + b_{10}u_n^2\delta + O((|u_n| + |v_n| + |\delta|)^4), \end{aligned}$$

$$\begin{aligned} a_1 &= -\frac{bcd^2}{cd^2 + b(-2+d)\alpha}, \ a_2 = \frac{bc^2d^2}{cd^2 + b(-2+d)\alpha}, \ a_3 = \frac{c^2(-2+d)\alpha}{cd^2 + b(-2+d)\alpha}, \\ a_4 &= -\frac{c^3(-2+d)\alpha}{3(cd^2 + b(-2+d)\alpha)}, \ a_5 = \frac{c^2(cd^2 - b(-2+d)\alpha)}{2(cd^2 + b(-2+d)\alpha)}, \ a_6 = \frac{c(-cd^2 + b(-2+d)\alpha)}{cd^2 + b(-2+d)\alpha}, \end{aligned}$$

$$a_7=\frac{b^2(3cd^2+b(-2+d)\alpha)}{6(cd^2+b(-2+d)\alpha)},\ a_8=-\frac{b\alpha}{cd+b\alpha},\ a_9=-\frac{c\alpha}{cd+b\alpha},$$
$$a_{10}=\frac{bc\alpha}{cd+b\alpha},\ a_{11}=\frac{b^2\alpha}{2cd+2b\alpha},\ a_{12}=\frac{c^2\alpha}{2cd+2b\alpha},$$

$$b_1=\frac{cd^2+b(-2+d)\alpha}{4},\ b_2=-\frac{d(cd^2+b(-2+d)\alpha)}{2\alpha},\ b_3=-\frac{(-3+d)(cd^2+b(-2+d)\alpha)^2}{24(-2+d)^2},$$
$$b_4=-\frac{d(4-5d+d^2)(cd^2+b(-2+d)\alpha)^2}{8(-2+d)^2\alpha^2},\ b_5=\frac{(2-4d+d^2)(cd^2+b(-2+d)\alpha)^2}{8(-2+d)^2\alpha},$$
$$b_6=\frac{(6-6d+d^2)(cd^3+b(-2+d)d\alpha)^2}{24(-2+d)^2\alpha^3},\ b_7=\frac{cd^4+b(-2+d)d^2\alpha}{4\alpha^2},$$
$$b_8=-\frac{(cd^2+b(-2+d)\alpha)^2}{8(-2+d)(cd+b\alpha)},\ b_9=\frac{d(cd^2+b(-2+d)\alpha)^2}{4(-2+d)\alpha(cd+b\alpha)},\ b_{10}=-\frac{(cd^3+b(-2+d)d\alpha)^2}{8(-2+d)\alpha^2(cd+b\alpha)}.$$

Next, the system (3.2) is diagonalized through the consideration of the following transformation:

$$\begin{bmatrix} u_n \\ v_n \end{bmatrix}=\begin{bmatrix} \frac{(-2+d)\alpha}{d^2} & \frac{2c\alpha}{cd^2-2b\alpha+bd\alpha} \\ 1 & 1 \end{bmatrix}\begin{bmatrix} e_n \\ f_n \end{bmatrix}. \tag{3.3}$$

Upon applying the mapping (3.3), the system (3.2) undergoes the alteration as follows:

$$\begin{bmatrix} e_{n+1} \\ f_{n+1} \end{bmatrix}=\begin{bmatrix} -1 & 0 \\ 0 & \xi \end{bmatrix}\begin{bmatrix} e_n \\ f_n \end{bmatrix}+\begin{bmatrix} \Gamma(e_n,f_n,\delta) \\ \Upsilon(e_n,f_n,\delta) \end{bmatrix}, \tag{3.4}$$

where

$$\xi=-\frac{c(-3+d)d^2+b(2-3d+d^2)\alpha}{cd^2+b(-2+d)\alpha},$$

$$\begin{aligned}\Gamma(e_n,f_n,\delta)&=c_1e_n^2+c_2e_n^3+c_3e_nf_n+c_4e_n^2f_n+c_5f_n^2+c_6f_n^3+c_7e_nf_n^2+c_8f_n\delta\\&\quad+c_9e_nf_n\delta+c_{10}e_n\delta+c_{11}f_n^2\delta+c_{12}e_n^2\delta+O((|e_n|+|f_n|+|\delta|)^4),\\ \Upsilon(e_n,f_n,\delta)&=d_1e_n^3+d_2e_n^2+d_3e_n^2f_n+d_4e_nf_n+d_5f_n^2+d_6f_n^3+d_7e_nf_n^2+d_8f_n\delta\\&\quad+d_9e_n\delta+d_{10}e_n^2\delta+d_{11}e_nf_n\delta+d_{12}f_n^2\delta+O((|e_n|+|f_n|+|\delta|)^4),\end{aligned}$$

where the values of coefficients are given in Appendix A. Next, assume that Q^C is the center manifold of (3.4) intended at origin in a close neighborhood of $\delta=0$. It can be approximated as follows:

$$Q^C=\left\{(e_n,f_n,\delta)\in\mathbb{R}_+^3\middle|f_n=p_1e_n^2+p_2e_n\delta+p_3\delta^2+O((|e_n|+|\delta|)^3)\right\},$$

where

$$p_1=\frac{d_2}{1-\xi},\ p_2=-\frac{d_9}{1+\xi},\ p_3=0.$$

As a result, the system (3.4) is limited to Q^C in the manner as follows:

$$\tilde{F} := e_{n+1} = -e_n + c_1 e_n^2 + c_{10} e_n \delta + \left(c_2 + \frac{c_3 d_2}{1-\xi}\right) e_n^3 - \left(\frac{c_8 d_9}{1+\xi}\right) e_n \delta^2 + \left(c_{12} + \frac{c_8 d_2}{1-\xi} - \frac{c_3 d_9}{1+\xi}\right) e_n^2 \delta + O\left((|e_n| + |\delta|)^4\right). \tag{3.5}$$

For the function (3.5) to go through PD bifurcation, it is necessary that the following two quantities possesses nonzero values:

$$l_1 = \tilde{F}_\delta \tilde{F}_{e_n e_n} + 2\tilde{F}_{e_n \delta}\Big|_{(0,0)} = 2c_{10}, \tag{3.6}$$

$$l_2 = \frac{1}{2}(\tilde{F}_{e_n e_n})^2 + \frac{1}{3}\tilde{F}_{e_n e_n e_n}\Big|_{(0,0)} = 2\left(c_1^2 + c_2 + \frac{c_3 d_2}{1-\xi}\right). \tag{3.7}$$

From the previous discussion, we get the following theorem:

Theorem 3.1. *Assume that condition (4-c) of Theorem 2.1 holds true. The system* (1.5) *experiences PD bifurcation at E_2 if l_1, l_2 given in* (3.6) *and* (3.7) *are nonzero and a fluctuates in a close neighborhood of $A_1 = \frac{2(-2+d)(cd+b\alpha)}{cd^2+b(-2+d)\alpha}$. Moreover, if $l_2 > 0$ (respectively, $l_2 < 0$), then a period-2 orbit of the system* (1.5) *emerges and it is stable (respectively, unstable).*

Next, we proceed to investigate the NS bifurcation at E_2 under condition (5-a) stated in Theorem 2.1. By applying a small perturbation δ ($|\delta| \lll 1$) to the bifurcation parameter around the critical value A_2, the system (1.5) is changed to

$$\begin{cases} x_{n+1} = x_n e^{(A_2+\delta) - b x_n - c y_n}, \\ y_{n+1} = y_n e^{d - \frac{\alpha y_n}{x_n}}. \end{cases} \tag{3.8}$$

We transform the fixed point E_2 to the origin by considering the change of variables $u_n = x_n - \frac{(a+\delta)\alpha}{cd+b\alpha}$, $v_n = y_n - \frac{(a+\delta)d}{cd+b\alpha}$. As a result, the system (3.8) is transformed into the following form:

$$\begin{bmatrix} u_{n+1} \\ v_{n+1} \end{bmatrix} = \begin{bmatrix} \frac{8c^2+2bc\alpha(1-2\delta)-b^2\alpha^2(1+\delta)}{(2c+b\alpha)(4c+b\alpha)} & -\frac{c\alpha(4c(1+\delta)+b\alpha(2+\delta))}{(2c+b\alpha)(4c+b\alpha)} \\ \frac{4}{\alpha} & -1 \end{bmatrix} \begin{bmatrix} u_n \\ v_n \end{bmatrix} + \begin{bmatrix} F(u_n, v_n) \\ G(u_n, v_n) \end{bmatrix}, \tag{3.9}$$

where

$$F(u_n, v_n) = a_1 u_n^2 + a_2 u_n^2 v_n + a_3 u_n v_n^2 + a_4 v_n^2 + a_5 v_n^3 + a_6 u_n^3 + a_7 u_n v_n + O((|u_n| + |v_n|)^4),$$
$$G(u_n, v_n) = b_1 v_n^3 + b_2 u_n^3 + b_3 u_n^2 v_n + b_4 u_n v_n^2 + O((|u_n| + |v_n|)^4),$$

$$a_1 = \frac{b(-16c^2 + 4bc\alpha(-2+\delta) + b^2\alpha^2\delta)}{2(2c+b\alpha)(4c+b\alpha)}, \quad a_2 = -\frac{bc(-16c^2 + 4bc\alpha(-2+\delta) + b^2\alpha^2\delta)}{2(2c+b\alpha)(4c+b\alpha)},$$
$$a_3 = \frac{c^2(8c^2 + 2bc\alpha(1-2\delta) - b^2\alpha^2(1+\delta))}{2(2c+b\alpha)(4c+b\alpha)}, \quad a_4 = \frac{c^2\alpha(4c(1+\delta) + b\alpha(2+\delta))}{2(2c+b\alpha)(4c+b\alpha)},$$
$$a_5 = -\frac{c^3\alpha(4c(1+\delta) + b\alpha(2+\delta))}{6(2c+b\alpha)(4c+b\alpha)}, \quad a_6 = -\frac{b^2(-24c^2 + b^2\alpha^2(-1+\delta) + 2bc\alpha(-7+2\delta))}{6(2c+b\alpha)(4c+b\alpha)},$$

$$a_7 = \frac{c(-8c^2 + b^2\alpha^2(1+\delta) + 2bc\alpha(-1+2\delta))}{(2c+b\alpha)(4c+b\alpha)},\ b_1 = \frac{(2c+b\alpha)^2}{6(\frac{4c+2b\alpha}{4c+b\alpha}+\delta)^2},$$
$$b_2 = -\frac{4(2c+b\alpha)^2}{3\alpha^3(\frac{4c+2b\alpha}{4c+b\alpha}+\delta)^2},\ b_3 = \frac{2(2c+b\alpha)^2}{\alpha^2(\frac{4c+2b\alpha}{4c+b\alpha}+\delta)^2},\ b_4 = -\frac{(2c+b\alpha)^2}{\alpha(\frac{4c+2b\alpha}{4c+b\alpha}+\delta)^2}.$$

The characteristic equation of the Jacobian matrix of system (3.9) estimated at origin is

$$\xi^2 - \alpha(\delta)\xi + \beta(\delta) = 0, \tag{3.10}$$

where

$$\alpha(\delta) = -\frac{b\alpha(4c(1+\delta) + b\alpha(2+\delta))}{(2c+b\alpha)(4c+b\alpha)},\ \beta(\delta) = \frac{b\alpha(1+\delta) + c(2+4\delta)}{2c+b\alpha}.$$

The complex solutions for (3.10) are calculated as:

$$\xi_{1,2} = \frac{\alpha(\delta)}{2} \pm \frac{i}{2}\sqrt{4\beta(\delta) - \alpha^2(\delta)}. \tag{3.11}$$

Moreover, we obtain

$$\left(\frac{d|\xi_1|}{d\delta}\right)_{\delta=0} = \left(\frac{d|\xi_2|}{d\delta}\right)_{\delta=0} = \frac{4c+b\alpha}{4c+2b\alpha} > 0.$$

Additionally, it is required that $\xi_{1,2}^k \neq 1$ when δ=0 for $k = 1,2,3,4$, which corresponds to $\alpha(0) \neq -2, 2, 0, 1$. We obtain

$$\alpha(0) = -\frac{2b\alpha}{4c+b\alpha} < 0.$$

Moreover, $\alpha(0) = -2$ is equivalent to $c = 0$, which is not possible. Next, to change (3.9) into normal form at $\delta = 0$, we use the following transformation:

$$\begin{bmatrix} u_n \\ v_n \end{bmatrix} = \begin{bmatrix} -\frac{2c\alpha}{4c+b\alpha} & 0 \\ -\frac{4c}{4c+b\alpha} & -\frac{1}{2}\sqrt{4 - \frac{4b^2\alpha^2}{(4c+b\alpha)^2}} \end{bmatrix} \begin{bmatrix} X_n \\ Y_n \end{bmatrix}. \tag{3.12}$$

Upon application of the mapping (3.12), the system (3.9) takes the following form:

$$\begin{bmatrix} X_{n+1} \\ Y_{n+1} \end{bmatrix} = \begin{bmatrix} -\frac{b\alpha}{4c+b\alpha} & -\frac{1}{2}\sqrt{4 - \frac{4b^2\alpha^2}{(4c+b\alpha)^2}} \\ \frac{1}{2}\sqrt{4 - \frac{4b^2\alpha^2}{(4c+b\alpha)^2}} & -\frac{b\alpha}{4c+b\alpha} \end{bmatrix} \begin{bmatrix} X_n \\ Y_n \end{bmatrix} + \begin{bmatrix} \Gamma(X_n, Y_n) \\ \Upsilon(X_n, Y_n) \end{bmatrix}, \tag{3.13}$$

where

$$\Gamma(X_n, Y_n) = c_1 X_n^2 Y_n + c_2 X_n Y_n^2 + c_3 X_n^2 + c_4 Y_n^2 + c_5 X_n Y_n + c_6 X_n^3 + c_7 Y_n^3 + O((|X_n| + |Y_n|)^4),$$
$$\Upsilon(X_n, Y_n) = d_1 X_n^2 Y_n + d_2 X_n Y_n + d_3 X_n Y_n^2 + d_4 X_n^2 + d_5 Y_n^2 + d_6 X_n^3 + d_7 Y_n^3 + O((|X_n| + |Y_n|)^4),$$

and

$$c_1 = 8\sqrt{2}c^2\frac{(c(2c+b\alpha))^{3/2}}{(4c+b\alpha)^3},\ c_2 = -\frac{4bc^3\alpha(2c+b\alpha)}{(4c+b\alpha)^3},\ c_3 = \frac{4c^2(2c+b\alpha)}{(4c+b\alpha)^2},$$

$$c_4=-\frac{4c^2(2c+b\alpha)}{(4c+b\alpha)^2},\ c_5=-\frac{2\sqrt{2}bc\alpha\sqrt{c(2c+b\alpha)}}{(4c+b\alpha)^2},\ c_6=\frac{2c^2(2c+b\alpha)^2(8c+b\alpha)}{3(4c+b\alpha)^3},$$
$$c_7=-\frac{1}{48}c^2(4-\frac{4b^2\alpha^2}{(4c+b\alpha)^2})^{3/2},\ d_1=-\frac{16c^4(2c+b\alpha)}{(4c+b\alpha)^3},\ d_2=\frac{4bc^2\alpha}{(4c+b\alpha)^2},$$
$$d_3=\frac{4\sqrt{2}bc^3\alpha\sqrt{c(2c+b\alpha)}}{(4c+b\alpha)^3},\ d_4=-\frac{4\sqrt{2}c^2\sqrt{c(2c+b\alpha)}}{(4c+b\alpha)^2},\ d_5=\frac{4\sqrt{2}c^2\sqrt{c(2c+b\alpha)}}{(4c+b\alpha)^2},$$
$$d_6=-\frac{2}{3}\sqrt{2}c\frac{(c(2c+b\alpha))^{3/2}(8c+b\alpha)}{(4c+b\alpha)^3},\ d_7=\frac{c(160c^4+176bc^3\alpha+72b^2c^2\alpha^2+14b^3c\alpha^3+b^4\alpha^4)}{3(4c+b\alpha)^3}.$$

The map (3.13) can undergo NS bifurcation if the following quantity is nonzero:

$$L=\Big(-Re\Big(\frac{(1-2\xi_1)\xi_2^2}{1-\xi_1}\tau_{20}\tau_{11}\Big)-\frac{1}{2}|\tau_{11}|^2-|\tau_{02}|^2+Re(\xi_2\tau_{21})\Big)_{\delta=0},\tag{3.14}$$

where

$$\tau_{20}=\frac{1}{8}\Big(\Gamma_{X_nX_n}-\Gamma_{Y_nY_n}+2\Upsilon_{X_nY_n}+i(\Upsilon_{X_nX_n}-\Upsilon_{Y_nY_n}-2\Gamma_{X_nY_n})\Big),$$
$$\tau_{11}=\frac{1}{4}\Big(\Gamma_{X_nX_n}+\Gamma_{Y_nY_n}+i(\Upsilon_{X_nX_n}+\Upsilon_{Y_nY_n})\Big),$$
$$\tau_{02}=\frac{1}{8}\Big(\Gamma_{X_nX_n}-\Gamma_{Y_nY_n}-2\Upsilon_{X_nY_n}+i(\Upsilon_{X_nX_n}-\Upsilon_{Y_nY_n}+2\Gamma_{X_nY_n})\Big),$$
$$\tau_{21}=\frac{1}{16}\Big(\Gamma_{X_nX_nX_n}+\Gamma_{X_nY_nY_n}+\Upsilon_{X_nX_nY_n}+\Upsilon_{Y_nY_nY_n}+i(\Upsilon_{X_nX_nX_n}+\Upsilon_{X_nY_nY_n}-\Gamma_{X_nX_nY_n}-\Gamma_{Y_nY_nY_n})\Big).$$

Therefore, the result derived from the above analysis is as follows:

Theorem 3.2. *Suppose that condition (5-a) of Theorem 2.1 holds true. If L given in* (3.14) *holds a nonzero value, then system* (1.5) *experiences NS bifurcation at E_2 as long as a fluctuates in a close neighborhood of $A_2=\frac{d(cd+b\alpha)}{cd^2+b(-1+d)\alpha}$. Furthermore, in instances where L is negative (alternatively, positive), the NS bifurcation encountered in system* (1.5) *at E_2 is categorized as supercritical (subcritical), giving rise to the presence of a unique closed invariant curve originating from E_2, that is, attracting (repelling).*

4. Chaos control

The aim of optimizing dynamical systems in order to meet particular performance criteria and minimize chaotic behavior is a highly desirable objective. Chaos control techniques are extensively employed in several fields of applied research and engineering. Historically, bifurcations and unstable oscillations have been regarded in a negative light within the field of mathematical biology due to their detrimental impact on the reproductive capacity of biological populations. It is possible to design a controller that may modify the bifurcation features of a nonlinear system in order to achieve specific desired dynamical attributes and effectively control chaos under the effects of PD and NS bifurcations. Multiple strategies exist for the purpose of managing chaos in a discrete-time system. This section is dedicated to examining two distinct control methods, namely, state feedback control and hybrid control approaches.

Initially, the state feedback control strategy, as described in references [35, 36], is employed to regulate the chaotic behavior of the system (1.5). The suggested methodology entails the conversion of the chaotic system into a piecewise linear system in order to obtain an optimal controller that effectively reduces the upper limit. Following this, the problem of optimization is carried out subject to certain constraints. The technique described above is utilized in order to attain stabilization of chaotic orbits situated at an unstable fixed point within the system (1.5). The controlled system under consideration for this purpose is as follows:

$$\begin{cases} x_{n+1} = x_n e^{a-bx_n-cy_n} - U_n, \\ y_{n+1} = y_n e^{d-\frac{\alpha y_n}{x_n}}, \end{cases} \tag{4.1}$$

where $U_n = \kappa_1\Big(x_n - \frac{a\alpha}{cd+b\alpha}\Big) + \kappa_2\Big(y_n - \frac{ad}{cd+b\alpha}\Big)$ is the feedback controlling force with feedback gains κ_1 and κ_2. Through simple calculations, it is obtained that for system (4.1) we have

$$J(E_2) = \begin{bmatrix} -\frac{cd(-1+\kappa_1)+b(-1+a+\kappa_1)\alpha}{cd+b\alpha} & -\kappa_2 - \frac{ac\alpha}{cd+b\alpha} \\ \frac{d^2}{\alpha} & 1-d \end{bmatrix}. \tag{4.2}$$

The matrix $J(E_2)$ has the following characteristic equation:

$$\xi^2 + K_1\xi + K_0 = 0, \tag{4.3}$$

where

$$K_1 = \frac{cd(-2+d+\kappa_1) + b(-2+a+d+\kappa_1)\alpha}{cd+b\alpha},$$
$$K_0 = \frac{cd(d^2\kappa_2 + \alpha - \kappa_1\alpha + d(-1+a+\kappa_1)\alpha) + b\alpha(d^2\kappa_2 - (-1+a+\kappa_1)\alpha + d(-1+a+\kappa_1)\alpha)}{\alpha(cd+b\alpha)}.$$

Let ξ_1 and ξ_2 be the roots of (4.3), then we have

$$\xi_1 + \xi_2 = -\frac{cd(-2+d+\kappa_1) + b(-2+a+d+\kappa_1)\alpha}{cd+b\alpha}, \tag{4.4}$$

$$\xi_1\xi_2 = \frac{cd(d^2\kappa_2 + \alpha - \kappa_1\alpha + d(-1+a+\kappa_1)\alpha) + b\alpha(d^2\kappa_2 - (-1+a+\kappa_1)\alpha + d(-1+a+\kappa_1)\alpha)}{\alpha(cd+b\alpha)}. \tag{4.5}$$

The lines of marginal stability are derived by solving $\xi_1 = \pm 1$ and $\xi_1\xi_2 = 1$. These conditions ensure that $|\xi_{1,2}| < 1$. Assume that $\xi_1\xi_2 = 1$, then Eq (4.5) implies that

$$L_1 : \Big(-1+d\Big)\kappa_1 + \Big(\frac{d^2}{\alpha}\Big)\kappa_2 + \frac{(-1+a)cd^2 + b(a(-1+d)-d)\alpha}{cd+b\alpha} = 0. \tag{4.6}$$

Next, we take $\xi_1 = 1$ and, utilizing Eqs (4.4) and (4.5), we obtain

$$L_2 : d\kappa_1 + \Big(\frac{d^2}{\alpha}\Big)\kappa_2 + ad = 0. \tag{4.7}$$

Next, we take $\xi_1 = -1$ and, utilizing Eqs (4.4) and (4.5), we obtain

$$L_3 : \Big(-2+d\Big)\kappa_1 + \Big(\frac{d^2}{\alpha}\Big)\kappa_2 + \frac{cd(4+(-2+a)d)+(-2+a)b(-2+d)\alpha}{cd+b\alpha} = 0. \tag{4.8}$$

The stable eigenvalues are enclosed within the triangular region bounded L_1, L_2 and L_3.

Next, we apply the hybrid control approach [37] for controlling chaos through both types of bifurcation effects. The hybrid control technique refers to a methodology that integrates the utilization of state feedback and parameter adjustment in order to achieve stabilization of unstable periodic orbits that are present within the chaotic attractor of a given system. The controlled system of (1.5), when the hybrid control approach is used, becomes

$$\begin{cases} x_{n+1} = \rho\Big(x_n e^{a-bx_n-cy_n}\Big) + (1-\rho)x_n, \\ y_{n+1} = \rho y_n e^{d-\frac{\alpha y_n}{x_n}} + (1-\rho)y_n, \end{cases} \tag{4.9}$$

where $\rho \in (0,1)$. The parameter ρ serves as a control parameter, which balances the influence of the original system (1.5) in comparison to the modified system (4.9). If the value of ρ is negative, it might suggest the reverse impact of the original system (1.5). If the value of ρ is more than 1, it suggests that the original system (1.5) has an intensifying impact on the modified system (4.9), perhaps resulting in impractical or unfeasible outcomes. Systems (4.9) and (1.5) share the same fixed points. We obtain

$$J(E_2) = \begin{bmatrix} 1-\frac{ab\alpha\rho}{cd+b\alpha} & -\frac{ac\alpha\rho}{cd+b\alpha} \\ \frac{d^2\rho}{\alpha} & 1-d\rho \end{bmatrix}, \tag{4.10}$$

then, its characteristic equation is as follows:

$$\xi^2 + K_1\xi + K_0 = 0, \tag{4.11}$$

where

$$\begin{aligned} K_1 &= \frac{cd(-2+d\rho)+b\alpha(-2+a\rho+d\rho)}{cd+b\alpha}, \\ K_0 &= \frac{b\alpha(-1+a\rho)(-1+d\rho)+cd(1+d\rho(-1+a\rho))}{cd+b\alpha}. \end{aligned}$$

Theorem 4.1. *The fixed point E_2 of the controlled system* (4.9) *is LAS if*

$$|K_1| < 1 + K_0 < 2.$$

5. Numerical examples

In this section, we provide empirical evidence to support our theoretical conclusions for system (1.5) through the implementation of numerical simulations. The numerical simulations will include the depiction of bifurcation diagrams, phase portraits, time series plots, and graphs illustrating the maximum Lyapunov exponent (MLE).

Example 5.1. *We assume that* $b = 0.5, c = 0.8, d = 2, \alpha = 2.5$, *then system* (1.5) *experiences NS bifurcation as a varies in small neighborhoods of* $a_2 \approx 1.280899$. *The positive fixed point is obtained as* $E_2 = (1.123596, 0.898876)$ *for* $a = 1.280899$. *The eigenvalues of* $J(E_2)$ *are* $\xi_{1,2}$=$-0.280899 \pm 0.959737i$ *with* $|\xi_{1,2}| = 1$. *Moreover, some careful calculations give*

$$\tau_{20} = 0.224618 - 0.084112i, \tau_{11} = -2.77556 \times 10^{-17} + 2.498 \times 10^{-16}i,$$
$$\tau_{02} = 0.14382 - 0.191947i, \tau_{21} = 0.449327 - 0.076779i.$$

Thus, it is obtained that $L = -0.257431 < 0$, *which proves the correctness of Theorem 3.2. The bifurcation diagrams of system* (1.5) *are given in Figure 1(a) and (b), while the MLE is plotted in Figure 1(c) by using initial conditions* $x_0 = 1.10$ *and* $y_0 = 0.90$ *and varying* $a \in [1.05, 2.25]$.

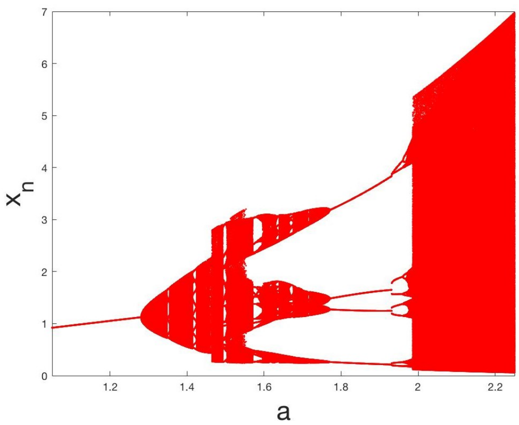

(a) Bifurcation diagram in (a, x_n) plane.

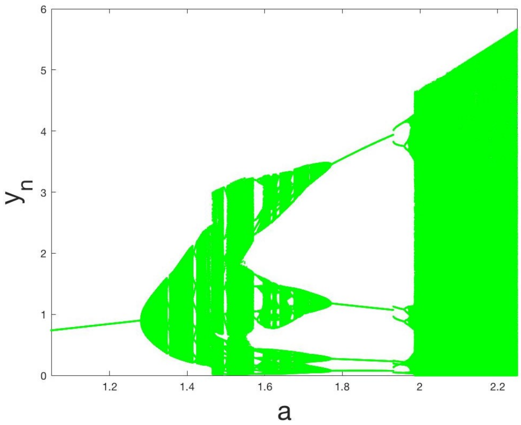

(b) Bifurcation diagram in (a, y_n) plane.

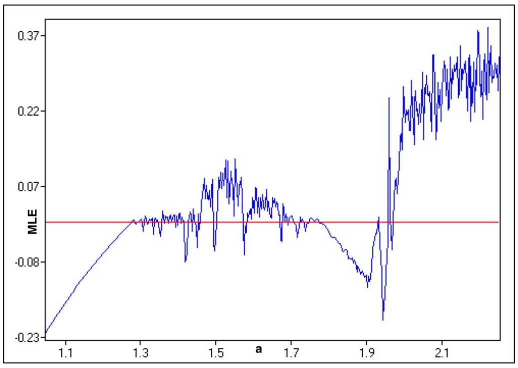

(c) MLE graph.

Figure 1. Bifurcation diagrams and MLE graph of system (1.5) with respect to a for $a \in [1.05, 2.25]$. Fixed parameter values are $b = 0.5, c = 0.8, d = 2, \alpha = 2.5$ and initial conditions are $x_0 = 1.10, y_0 = 0.90$.

Next, Figure 2(a)–(f) show phase portraits of system (1.5) *for various values of a. The positive fixed point* E_2 *remains stable when* $a < 1.280899$. *However, owing to an NS bifurcation, it loses stability at* $a = 1.280899$. *This results in the formation of an invariant closed curve, the radius of which expands as a grows. Furthermore, the MLE graph demonstrates that negative values of the MLE indicate a range of periodic orbits. For instance, orbit-7 in Figure 2(d), orbit-11 in Figure 2(f), orbit-15 in*

Figure 2(h), orbit-4 in Figure 2(l) and orbit-8 in Figure 2(m) exhibit this behavior. Conversely, positive MLE values suggest that the system is chaotic. Figure 2(o) and (p) exhibit the presence of strange attractors, indicating the chaotic character that results from positive MLE values.

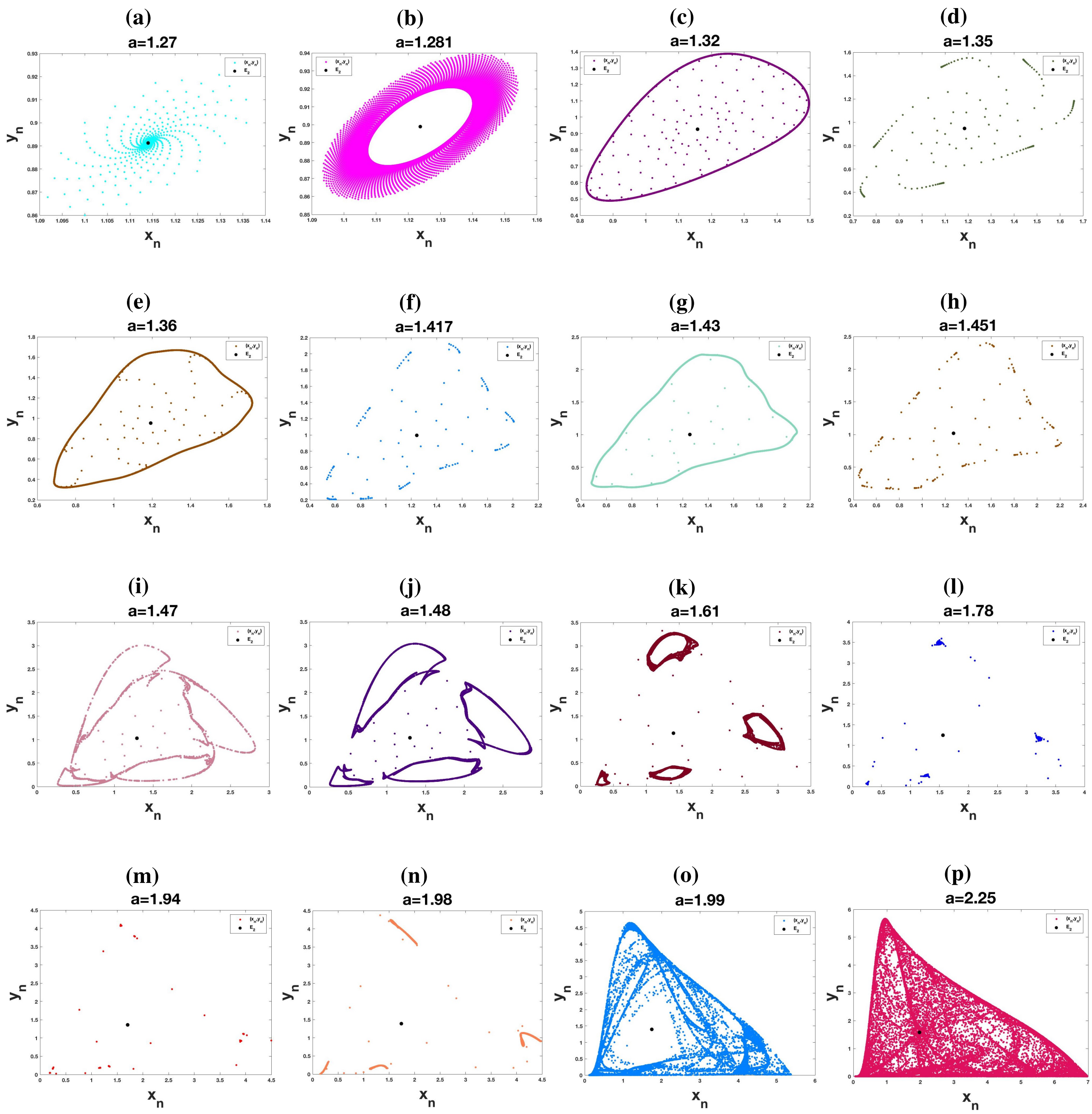

Figure 2. Phase portraits of (1.5) for various values of a and fixing $b = 0.5, c = 0.8, d = 2, \alpha = 2.5, x_0 = 1.10, y_0 = 0.90$.

Example 5.2. *We assume that* $b = 0.5, c = 0.8, d = 3.15, \alpha = 2.5$, *then system* (1.5) *experiences both PD bifurcation and NS bifurcation as a varies in small neighborhoods of* $A_1 \approx 0.924857$ *and*

$A_2 \approx 1.11764$, respectively. The positive fixed point is obtained as $E_2 = (0.613301, 0.772759)$ for $a = A_1$. The eigenvalues of $J(E_2)$ are $\xi_1 = -1$ and $\xi_2 = -0.45665$ with $|\xi_2| \neq 1$. The positive fixed point is obtained as $E_2 = (0.741142, 0.933838)$ for $a = A_2$. The eigenvalues of $J(E_2)$ are $\xi_{1,2}$=$-0.760285 \pm 0.649589i$ with $|\xi_{1,2}| = 1$. The bifurcation diagrams of system (1.5) are given in Figure 3(a) and (b), while the MLE is plotted in Figure 3(c) by using initial conditions $x_0 = 0.60$ and $y_0 = 0.75$ and varying a.

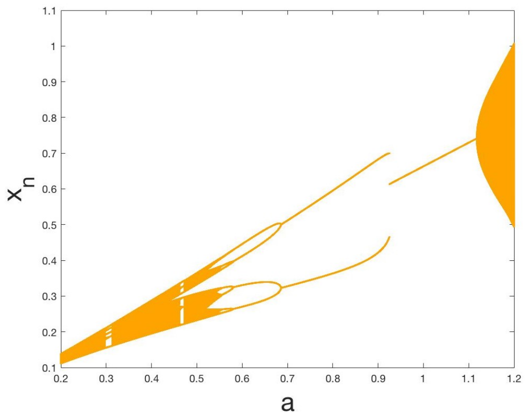

(a) Bifurcation diagram in (a, x_n) plane.

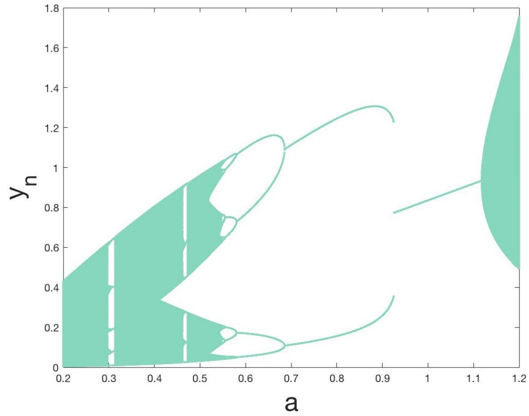

(b) Bifurcation diagram in (a, y_n) plane.

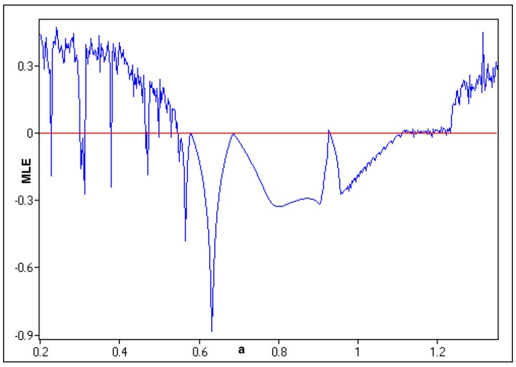

(c) MLE graph.

Figure 3. Bifurcation diagrams of system (1.5) with respect to a for $a \in [0.20, 1.20]$ and MLE graph for $a \in [0.20, 1.35]$. Fixed parameter values are $b = 0.5, c = 0.8, d = 3.15, \alpha = 2.5$ and initial conditions are $x_0 = 0.60, y_0 = 0.75$.

Next, Figure 4(a)–(l) show phase portraits of system (1.5) for various values of a. One can observe that E_2 is LAS for $0.924857 < a < 1.11764$, but loses stability at $a = 0.924857$ when the system (1.5) experiences PD bifurcation. For $a \geq 1.11764$, the system (1.5) experiences NS bifurcation and an invariant curve emerges from E_2, the radius of which grows as a grows. It leads to a strange chaotic attractor presented in Figure 4(l).

Therefore, it can be concluded that the positive fixed point E_2 of the system (1.5) exhibits stability when the growth rate of the prey population falls within the range (A_1, A_2). When the growth rate of the prey falls below the threshold value of A_1, it experiences difficulties in maintaining its population against predation, leading to a reduction that subsequently affects the survival of predators that rely on it. When the growth rate exceeds the value of A_2, rapid growth sustains predators initially but carries *the potential for resource exhaustion, therefore affecting both prey and predators over a long period of time.*

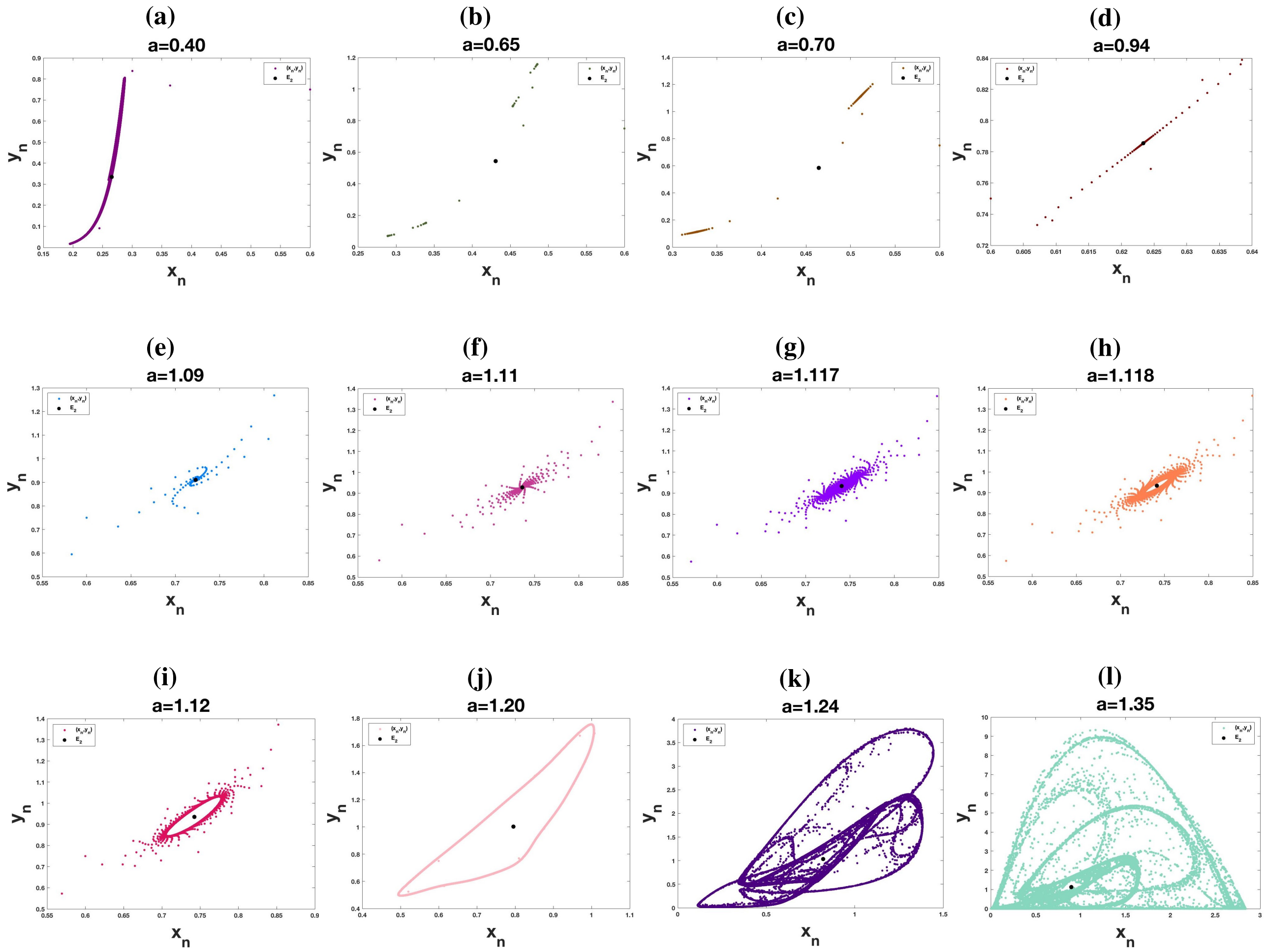

Figure 4. Phase portraits of (1.5) for various values of a and fixing $b = 0.5, c = 0.8$, $d = 3.15, \alpha = 2.5, x_0 = 0.60, y_0 = 0.75$.

Subsequently, our objective is to assess the effectiveness of the feedback control strategy. Given the values $a = 1.15, b = 0.5, c = 0.8, d = 3.15,$ *and* $\alpha = 2.5$, *together with the initial conditions* $x_0 = 0.60$ *and* $y_0 = 0.75$ *for the controlled system* (4.1)*, the marginal stability lines may be determined as follows:*

$$L_1 : \kappa_2 = -0.022978 - 0.541698\kappa_1,$$

$$L_2 : \kappa_2 = -0.912698 - 0.793651\kappa_1,$$

and

$$L_3 : \kappa_2 = -0.141068 - 0.289746\kappa_1.$$

The stability region of system (4.1) *is shown in Figure 5(a), which is bounded by lines* L_1, L_2 *and* L_3. *The instability of the fixed point* E_2 *of system* (1.5) *has been shown for the specified parametric values. The system described by Eq* (4.1) *is analyzed using feedback gains* $\kappa_1 = -3.01$ *and* $\kappa_2 = 1.60$. *Figure 5* *illustrates the graph of* x_n *as shown in Figure 5(c),* y_n *as shown in Figure 5(d), and the phase portrait as presented in Figure 5(b) for the system* (4.1). *Hence, it may be inferred that the use of the feedback control approach seems to be efficacious in managing bifurcation and chaos.*

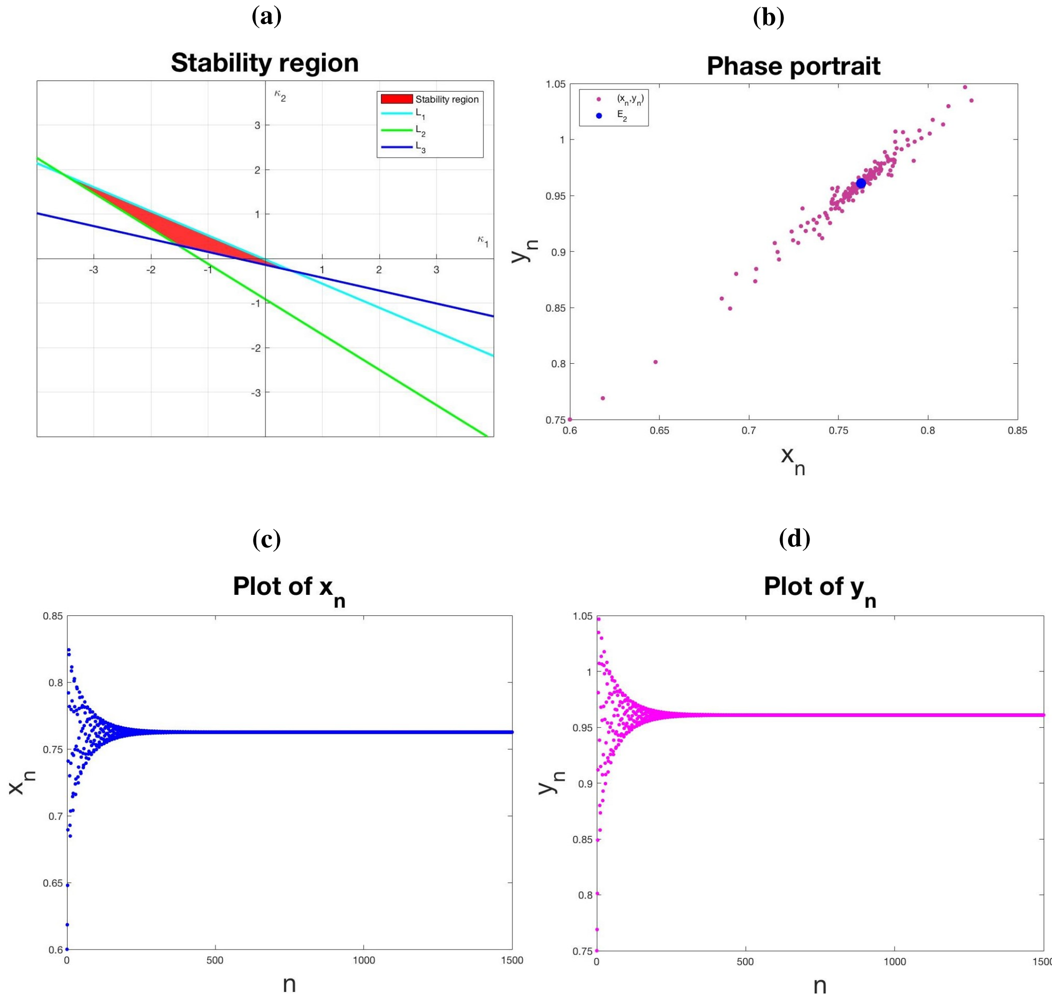

Figure 5. Stability region, phase portrait, and time series plots of system (4.1) using a=1.15, $b = 0.5, c = 0.8, d = 3.15, \alpha = 2.5, \kappa = -3.01, \kappa_2 = 1.60$ and initial conditions are x_0=0.60, $y_0 = 0.75$.

The effectiveness of the hybrid control strategy will now be assessed. We assume $\rho = 0.95$, b=0.5, $c = 0.8, d = 3.15, \alpha = 2.5$ *and vary* a *for the controlled system* (4.9). *If* $0.897012 < a < 1.183794$, *the positive fixed point* E_2 *is LAS. One can observe that the stability region has been expanded. The bifurcation diagrams are presented in Figure 6(a) and (b) by using initial conditions* $x_0 = 0.60$, y_0=0.75 *and varying* $a \in [0.20, 1.20]$.

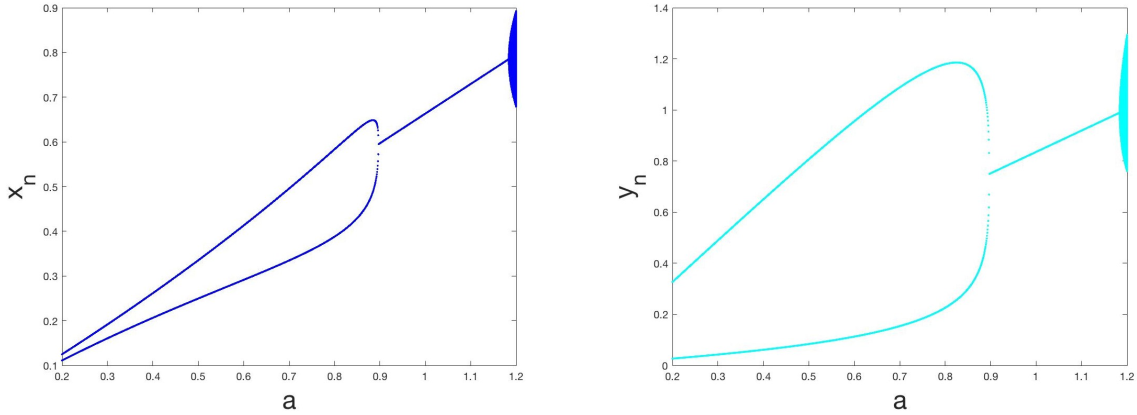

(a) Bifurcation diagram in (a, x_n) plane of system (4.9).

(b) Bifurcation diagram in (a, y_n) plane of system (4.9).

Figure 6. Bifurcation diagrams of system (4.9) by fixing $\rho = 0.95, b = 0.5, c = 0.8, d = 3.15$, $\alpha = 2.5, x_0 = 0.60, y_0 = 0.75$ and varying $a \in [0.20, 1.20]$.

6. Conclusions

Our study focused on a discrete-time system, which provided a more accurate depiction of animal dynamics in seasonal reproduction with nonoverlapping generations. These discrete systems, in comparison to continuous-time systems, displayed more detailed and rich dynamical patterns, making them more attractive. When discretizing continuous systems, it was critical to use proper numerical approaches. In this paper, we used the piecewise constant argument methodology to discretize the system (1.1), leading to a discrete system (1.5) that consistently preserved positive solutions. This approach presented a benefit in comparison to the Euler method, which was susceptible to producing negative solutions, thereby posing challenges for population systems. This study conducted a comprehensive analysis of the existence and stability of fixed points, focusing specifically on local bifurcations that occur at the positive fixed point. It was observed that our system (1.5) undergoes bifurcations in both PD and NS at a positive fixed point, whereas prior investigations [31] only reported NS bifurcations. Hybrid control and feedback control techniques were employed to effectively manage bifurcation and disorder within the system denoted as (1.5). In order to validate our theoretical findings, we employed numerical simulations that incorporated a range of graphical representations, such as time series plots, phase portraits, bifurcation diagrams, and MLE graphs.

It can be inferred that the stability of the positive fixed point E_2 is maintained when the prey population growth rate lies within the interval (A_1, A_2). In situations where the prey's growth rate fell below a certain threshold value denoted as A_1, it encountered challenges in sustaining its population in the face of predation, resulting in a decline that ultimately impacts the viability of predators dependent on it. When the growth rate exceeded the value of A_2, rapid growth sustained predators initially but carried the potential for resource exhaustion, therefore affecting both prey and predators over a long period of time.

Use of AI tools declaration

The authors declare they have not used Artificial Intelligence (AI) tools in the creation of this article.

Acknowledgments

This study is supported via funding from Prince Sattam bin Abdulaziz University project number (PSAU/2023/R/1445).

Conflict of interest

All authors declare no conflicts of interest in this paper.

References

1. A. Kashyap, Q. Zhu, H. Sarmah, D. Bhattacharjee, Dynamical study of a predator-prey system with Michaelis-Menten type predator-harvesting, *Int. J. Biomath.*, **16** (2023), 2250135. http://dx.doi.org/10.1142/S1793524522501352
2. M. Ghori, P. Naik, J. Zu, Z. Eskandari, M. Naik, Global dynamics and bifurcation analysis of a fractional-order SEIR epidemic model with saturation incidence rate, *Math. Method. Appl. Sci.*, **45** (2022), 3665–3688. http://dx.doi.org/10.1002/mma.8010
3. W. Lu, Y. Xia, Multiple periodicity in a predator-prey model with prey refuge, *Mathematics*, **10** (2022), 421. http://dx.doi.org/10.3390/math10030421
4. A. Matouk, Chaos and bifurcations in a discretized fractional model of quasi-periodic plasma perturbations, *Int. J. Nonlin. Sci. Num.*, **23** (2022), 1109–1127. http://dx.doi.org/10.1515/ijnsns-2020-0101
5. E. González-Olivares, A. Rojas-Palma, Limit cycles in a Gause-type predator-prey model with sigmoid functional response and weak Allee effect on prey, *Math. Method. Appl. Sci.*, **35** (2012), 963–975. http://dx.doi.org/10.1002/mma.2509
6. A. Elsadany, Q. Din, S. Salman, Qualitative properties and bifurcations of discrete-time Bazykin-Berezovskaya predator-prey model, *Int. J. Biomath.*, **13** (2020), 2050040. http://dx.doi.org/10.1142/S1793524520500400
7. D. Sen, S. Ghorai, M. Banerjee, A. Morozov, Bifurcation analysis of the predator-prey model with the allee effect in the predator, *J. Math. Biol.*, **84** (2022), 7. http://dx.doi.org/10.1007/s00285-021-01707-x
8. A. Suleman, R. Ahmed, F. Alshammari, N. Shah, Dynamic complexity of a slow-fast predator-prey model with herd behavior, *AIMS Mathematics*, **8** (2023), 24446–24472. http://dx.doi.org/10.3934/math.20231247
9. A. Lotka, Elements of physical biology, *Nature*, **116** (1925), 461. http://dx.doi.org/10.1038/116461b0

10. V. Volterra, Fluctuations in the abundance of a species considered mathematically, *Nature*, **118** (1926), 558–560. http://dx.doi.org/10.1038/118558a0

11. P. Leslie, Some further notes on the use of matrices in population mathematics, *Biometrika*, **35** (1948), 213–245. http://dx.doi.org/10.2307/2332342

12. P. Leslie, A stochastic model for studying the properties of certain biological systems by numerical methods, *Biometrika*, **45** (1958), 16–31. http://dx.doi.org/10.2307/2333042

13. N. Britton, *Essential mathematical biology*, London: Springer, 2003. http://dx.doi.org/10.1007/978-1-4471-0049-2

14. M. Zhao, C. Li, J. Wang, Complex dynamic behaviors of a discrete-time predator-prey system, *J. Appl. Anal. Comput.*, **7** (2017), 478–500. http://dx.doi.org/10.11948/2017030

15. S. Rana, Dynamics and chaos control in a discrete-time ratio-dependent Holling-Tanner model, *J. Egypt. Math. Soc.*, **27** (2019), 48. http://dx.doi.org/10.1186/s42787-019-0055-4

16. P. Baydemir, H. Merdan, E. Karaoglu, G. Sucu, Complex dynamics of a discrete-time prey-predator system with Leslie type: Stability, bifurcation analyses and chaos, *Int. J. Bifurcat. Chaos*, **30** (2020), 2050149. http://dx.doi.org/10.1142/s0218127420501497

17. S. Akhtar, R. Ahmed, M. Batool, N. Shah, J. Chung, Stability, bifurcation and chaos control of a discretized Leslie prey-predator model, *Chaos Soliton. Fract.*, **152** (2021), 111345. http://dx.doi.org/10.1016/j.chaos.2021.111345

18. P. Naik, Z. Eskandari, H. Shahraki, Flip and generalized flip bifurcations of a two-dimensional discrete-time chemical model, *Mathematical Modelling and Numerical Simulation with Applications*, **1** (2021), 95–101. http://dx.doi.org/10.53391/mmnsa.2021.01.009

19. Z. Eskandari, Z. Avazzadeh, R. Ghaziani, B. Li, Dynamics and bifurcations of a discrete-time Lotka-Volterra model using nonstandard finite difference discretization method, *Math. Method. Appl. Sci.*, in press. http://dx.doi.org/10.1002/mma.8859

20. P. Naik, Z. Eskandari, Z. Avazzadeh, J. Zu, Multiple bifurcations of a discrete-time prey-predator model with mixed functional response, *Int. J. Bifurcat. Chaos*, **32** (2022), 2250050. http://dx.doi.org/10.1142/s021812742250050x

21. P. Naik, Z. Eskandari, A. Madzvamuse, Z. Avazzadeh, J. Zu, Complex dynamics of a discrete-time seasonally forced SIR epidemic model, *Math. Method. Appl. Sci.*, **46** (2023), 7045–7059. http://dx.doi.org/10.1002/mma.8955

22. W. Liu, D. Cai, Bifurcation, chaos analysis and control in a discrete-time predator-prey system, *Adv. Differ. Equ.*, **2019** (2019), 11. http://dx.doi.org/10.1186/s13662-019-1950-6

23. Y. Li, F. Zhang, X. Zhuo, Flip bifurcation of a discrete predator-prey model with modified Leslie-Gower and Holling-type iii schemes, *Math. Biosci. Eng.*, **17** (2020), 2003–2015. http://dx.doi.org/10.3934/mbe.2020106

24. Rajni, B. Ghosh, Multistability, chaos and mean population density in a discrete-time predator-prey system, *Chaos Soliton. Fract.*, **162** (2022), 112497. http://dx.doi.org/10.1016/j.chaos.2022.112497

25. A. Yousef, A. Algelany, A. Elsadany, Codimension one and codimension two bifurcations in a discrete Kolmogorov type predator-prey model, *J. Comput. Appl. Math.*, **428** (2023), 115171. http://dx.doi.org/10.1016/j.cam.2023.115171

26. A. Khan, I. Alsulami, Complicate dynamical analysis of a discrete predator-prey model with a prey refuge, *AIMS Mathematics*, **8** (2023), 15035–15057. http://dx.doi.org/10.3934/math.2023768
27. A. Tassaddiq, M. Shabbir, Q. Din, H. Naaz, Discretization, bifurcation, and control for a class of predator-prey interactions, *Fractal Fract.*, **6** (2022), 31. http://dx.doi.org/10.3390/fractalfract6010031
28. S. Lin, F. Chen, Z. Li, L. Chen, Complex dynamic behaviors of a modified discrete Leslie-Gower predator-prey system with fear effect on prey species, *Axioms*, **11** (2022), 520. http://dx.doi.org/10.3390/axioms11100520
29. P. Naik, Z. Eskandari, M. Yavuz, J. Zu, Complex dynamics of a discrete-time Bazykin-Berezovskaya prey-predator model with a strong Allee effect, *J. Comput. Appl. Math.*, **413** (2022), 114401. http://dx.doi.org/10.1016/j.cam.2022.114401
30. R. Ahmed, M. Rafaqat, I. Siddique, M. Arefin, Complex dynamics and chaos control of a discrete-time predator-prey model, *Discrete Dyn. Nat. Soc.*, **2023** (2023), 8873611. http://dx.doi.org/10.1155/2023/8873611
31. A. Khan, I. Alsulami, Discrete Leslie's model with bifurcations and control, *AIMS Mathematics*, **8** (2023), 22483–22506. http://dx.doi.org/10.3934/math.20231146
32. A. Luo, *Regularity and complexity in dynamical systems*, New York: Springer, 2012. http://dx.doi.org/10.1007/978-1-4614-1524-4
33. J. Guckenheimer, P. Holmes, *Nonlinear oscillations, dynamical systems, and bifurcations of vector fields*, New York: Springer, 1983. http://dx.doi.org/10.1007/978-1-4612-1140-2
34. S. Wiggins, *Introduction to applied nonlinear dynamical systems and chaos*, New York: Springer, 1990. http://dx.doi.org/10.1007/978-1-4757-4067-7
35. G. Chen, X. Dong, *From chaos to order: methodologies, perspectives and applications*, Singapore: World Scientific, 1998. http://dx.doi.org/10.1142/3033
36. C. Lei, X. Han, W. Wang, Bifurcation analysis and chaos control of a discrete-time prey-predator model with fear factor, *Math. Biosci. Eng.*, **19** (2022), 6659–6679. http://dx.doi.org/10.3934/mbe.2022313
37. X. Luo, G. Chen, B. Wang, J. Fang, Hybrid control of period-doubling bifurcation and chaos in discrete nonlinear dynamical systems, *Chaos Soliton. Fract.*, **18** (2003), 775–783. http://dx.doi.org/10.1016/s0960-0779(03)00028-6

Appendix A.

$$c_1 = -\frac{2c(cd^2 + b(-2+d)\alpha)}{c(-4+d)d^2 + b(-2+d)^2\alpha},\ c_2 = \frac{(cd^2 + b(-2+d)\alpha)^2(cd^2(16-24d+4d^2+d^3) + b(-2+d)^4\alpha)}{6(-2+d)^2d^4(c(-4+d)d^2 + b(-2+d)^2\alpha)},$$

$$c_3 = -\frac{c(cd^3 + b(-4+d^2)\alpha)}{c(-4+d)d^2 + b(-2+d)^2\alpha},\ c_4 = \frac{2c(-1+d)(cd^2 + b(-2+d)\alpha)(c(-2+d)d^2 + b(-2-2d+d^2)\alpha)}{(-2+d)d^2(c(-4+d)d^2 + b(-2+d)^2\alpha)},$$

$$c_5 = -\Big(cd^2(c^3d^4(12-6d+d^2)+bc^2d^2(-16+36d-18d^2+3d^3)\alpha+3b^2c(-2+d)^3d\alpha^2+b^3(-2+d)^3\alpha^3)\Big)$$
$$\Big/\Big(2(cd^2+b(-2+d)\alpha)^2(c(-4+d)d^2+b(-2+d)^2\alpha)\Big),$$

$$c_6 = \Big(cd^2(cd+b\alpha)^2(c^3d^4(8+8d-5d^2+d^3)+bc^2(-2+d)^2d^2(6-7d+3d^2)\alpha+b^2c(-2+d)^2(-12+12d$$
$$-11d^2+3d^3)\alpha^2+b^3(-3+d)(-2+d)^3\alpha^3)\Big)\Big/\Big(12(cd^2+b(-2+d)\alpha)^3(c(-4+d)d^2+b(-2+d)^2\alpha)\Big),$$

$$c_7 = \Big(c\Big(3c^3d^4(8-4d+d^2)+bc^2d^2(-40+72d-40d^2+9d^3)\alpha+b^2cd(-48+72d-44d^2+9d^3)\alpha^2$$
$$+b^3(-8+24d-16d^2+3d^3)\alpha^3\Big)\Big)\Big/\Big(4(cd^2+b(-2+d)\alpha)(c(-4+d)d^2+b(-2+d)^2\alpha)\Big),$$

$$c_8 = -\frac{cd^3}{c(-4+d)d^2+b(-2+d)^2\alpha},\ c_9 = \frac{2cd(cd^2+b(-2+d)\alpha)}{c(-4+d)d^2+b(-2+d)^2\alpha},$$

$$c_{10} = -\frac{(cd^2+b(-2+d)\alpha)^2}{(cd+b\alpha)(c(-4+d)d^2+b(-2+d)^2\alpha)},\ c_{11} = \frac{cd^2(cd+b\alpha)(cd^3+b(-2+d)^2\alpha)}{4(cd^2+b(-2+d)\alpha)(c(-4+d)d^2+b(-2+d)^2\alpha)},$$

$$c_{12} = \frac{(cd^2+b(-2+d)\alpha)^2(cd^3+b(-2+d)^2\alpha)}{2(-2+d)d^2(cd+b\alpha)(c(-4+d)d^2+b(-2+d)^2\alpha)},$$

$$d_1 = -\frac{(8-11d+3d^2)(cd^2+b(-2+d)\alpha)^3}{3(-2+d)d^4(c(-4+d)d^2+b(-2+d)^2\alpha)},\ d_2 = \frac{(-2+d)(cd^2+b(-2+d)\alpha)^2}{c(-4+d)d^4+b(-2+d)^2d^2\alpha},$$

$$d_3 = -\frac{(cd^2+b(-2+d)\alpha)^2(cd(8-7d+2d^2)+b(4-7d+2d^2)\alpha)}{2d^3(c(-4+d)d^2+b(-2+d)^2\alpha)},$$

$$d_4 = \frac{(c^2d^3(8-5d+d^2)+bc(-2+d)^2d(-3+2d)\alpha+b^2(-2+d)^3\alpha^2)}{c(-4+d)d^3+b(-2+d)^2d\alpha},$$

$$d_5 = \Big(c^4d^6(8+8d-6d^2+d^3)+4bc^3d^4(4-12d+16d^2-7d^3+d^4)\alpha+2b^2c^2(-2+d)^2d^2(-4+12d$$
$$-12d^2+3d^3)\alpha^2+4b^3c(-2+d)^4(-1+d)d\alpha^3+b^4(-2+d)^5\alpha^4\Big)$$
$$\Big/\Big(4(cd^2+b(-2+d)\alpha)^2(c(-4+d)d^2+b(-2+d)^2\alpha)\Big),$$

$$d_6 = -\Big(cd+b\alpha)^2(c^4d^6(64-44d+22d^2-7d^3+d^4)+2bc^3d^4(-96+164d-130d^2+62d^3$$

$$-17d^4+2d^5)\alpha+6b^2c^2(-2+d)^3d^2(-6+6d-4d^2+d^3)\alpha^2+2b^3c(-2+d)^4(-6+6d-7d^2+2d^3)\alpha^3$$
$$+b^4(-3+d)(-2+d)^5\alpha^4)\Big)\Big/\Big(24(cd^2+b(-2+d)\alpha)^3(c(-4+d)d^2+b(-2+d)^2\alpha\Big),$$

$$d_7=-\Big(c^4d^7(28-16d+3d^2)+4bc^3d^4(16-40d+44d^2-19d^3+3d^4)\alpha+2b^2c^2(-2+d)^2d^2(-12+28d$$
$$-30d^2+9d^3)\alpha^2+4b^3c(-2+d)^2d(-8+16d-13d^2+3d^3)\alpha^3+b^4(-2+d)^3(4-10d+3d^2)\alpha^4)\Big)$$
$$\Big/\Big(8d^2(cd^2+b(-2+d)\alpha)(c(-4+d)d^2+b(-2+d)^2\alpha)\Big),$$

$$d_8=\frac{cd^3}{c(-4+d)d^2+b(-2+d)^2\alpha},\ d_9=\frac{(cd^2+b(-2+d)\alpha)^2}{(cd+b\alpha)(c(-4+d)d^2+b(-2+d)^2\alpha)},$$

$$d_{10}=-\frac{(cd^2+b(-2+d)\alpha)^3}{d^2(cd+b\alpha)(c(-4+d)d^2+b(-2+d)^2\alpha)},\ d_{11}=-\frac{(cd^2+b(-2+d)\alpha)(cd^3+b(-2+d)^2\alpha)}{2(c(-4+d)d^3+b(-2+d)^2d\alpha)},$$

$$d_{12}=-\frac{(cd+b\alpha)(c^2d^4(8-4d+d^2)+2bc(-2+d)^3d^2\alpha+b^2(-2+d)^4\alpha^2)}{8(cd^2+b(-2+d)\alpha)(c(-4+d)d^2+b(-2+d)^2\alpha)}.$$

AIMS Press